

## Supporting Information

### Edge-directed Rapid Chiral Assembly of Gold Nanorods by 2D Hexagonal Nanosheets of Helical Poly(phenylacetylene)s and the Synergistic Communication of Circular Polarized Luminescence

Peiyao Yu,<sup>†a</sup> Wenjing Zhao,<sup>†a, b</sup> Yihan Huang,<sup>a</sup> Hua Zeng,<sup>a</sup> Xinhua Wan,<sup>a</sup> and Jie Zhang<sup>\*a</sup>

## 1. Experimental Section

### 1.1 Materials

HAuCl<sub>4</sub> (98%, Innochem), cetyltrimethylammonium bromide (CTAB, 98%, Sigma-Aldrich), sodium borohydride (NaBH<sub>4</sub>, 98%, Acros), silver nitrate (AgNO<sub>3</sub>, 99%, Sigma-Aldrich), *L*-ascorbic acid (AA, 99%, Adamas), trisodium citrate (99%, Alfa Aesar), thiol PEG (E350:  $M_w = 350$  g/mol, E1k:  $M_w = 1000$  g/mol, E2k:  $M_w = 2000$  g/mol, E5k:  $M_w = 5000$  g/mol, Aladin), tetrahydrofuran (THF, HPLC, ThermoFisher), ethanol (EtOH, HPLC, Concord Technology (Tianjin) Co.)

### 1.2 The synthesis of gold nanorods (GNRs) and gold nanoparticles (GNPs)

GNRs were prepared by a seed-mediated growth approach.<sup>[1]</sup> A seed solution was firstly prepared. 250  $\mu$ L of 10 mM HAuCl<sub>4</sub> was added to 7.5 mL of a 100 mM CTAB solution at 30 °C. After mixing, 600  $\mu$ L of 10 mM NaBH<sub>4</sub> solution was added, followed by rapid stirring for 3 min. The Au seed solution was stored at 30 °C for 2 h. Secondly, a growth solution was prepared. 4 ml of 10 mM HAuCl<sub>4</sub>, 10 mM AgNO<sub>3</sub>, 480  $\mu$ L of 100 mM AA and 96  $\mu$ L of CTAB-capped gold seed solution were added into 80 ml of 100 mM CTAB solution. The solution was reacted for 24 h. GNRs were centrifuged three times (9000 rpm, 10 min) and redispersed in 1 mM CTAB solution. The amount of AgNO<sub>3</sub> for G1 is 240  $\mu$ L, G2 is 320  $\mu$ L, G3 is 400 $\mu$ L, G4 is 480  $\mu$ L and G5 is 560  $\mu$ L.<sup>[2]</sup>

GNPs were prepared by reduction of HAuCl<sub>4</sub> using trisodium citrate by previously reported approach.<sup>[3]</sup> 1.5 mL of 1 wt% trisodium citrate solution was quickly added to a boiling solution of 100 mL of 0.25 mM HAuCl<sub>4</sub>. The solution was refluxed for 20 min. The reaction solution was subsequently cooled down to room temperature.

### 1.3 Surface modification of GNRs and GNPs

1 mL of 0.1 wt% PEG and 1 mL of GNRs or GNPs were mixed and stirred overnight, and then centrifuged at 9000 rpm for 5 minutes. 1997  $\mu\text{L}$  of the supernatant was discarded, and 1997  $\mu\text{L}$  of  $\text{H}_2\text{O}$  was added. Repeat this process once, and retain 3  $\mu\text{L}$  of the concentrated solution. G2-E5k-E1k was modified twice. 1 mL of 0.1 wt% E1k and 3  $\mu\text{L}$  of G2-E5k were mixed and stirred 1 h. The next steps are the same as before.

### 1.4 The self-assembly of PPA

Synthesis of PPAs (P1, P2 and P3) and preparation of hexagonal assemblies were reported previously.<sup>[4]</sup> P1 assemblies: the solution of P1 in THF (0.40 mg/mL, 1 mL in 5 mL vial) was added with EtOH dropwise without stirring at 25°C. When the EtOH fraction reached 33% (500  $\mu\text{L}$ ). When the P1 assembly is placed for 1 hour, 24 h or 3 days, assemblies of different diameters can be obtained. P2 assemblies: the EtOH fraction reached 66% (1500  $\mu\text{L}$ ). P3 assemblies: the EtOH fraction reached 13% (150  $\mu\text{L}$ ).

Synthesis of P4 and preparation of fiber assemblies were also reported previously.<sup>[5]</sup> P4 assemblies: P4 was dissolved in THF (0.15 mg/mL, 1 mL in 5 mL vial) at 25°C.

### 1.5 Preparation of PPAs/GNRs (or GNPs) co-assemblies

The co-assemblies were obtained by blending the PPAs and GNRs (or GNPs) concentrated solution. Taking *R*-P1/G2-E1k (the concentration of *R*-P1 is 0.4 mg/mL) as an example. Add 3  $\mu\text{L}$   $\text{H}_2\text{O}$  to 3  $\mu\text{L}$  G2-E1k, followed by adding 100  $\mu\text{L}$  THF/EtOH (THF/EtOH = 2/1 (*V/V*)). The co-assembly can be obtained by adding the G2-E1k organic solution into the solution of *R*-P1 assemblies and stirring.

### 1.6 Computer simulations

#### 1.6.1 Simulation of PPAs:

The molecular modeling and molecular mechanics calculations were conducted in the Material Studio10 software (version 5.0; Accelrys Software Inc.). The methods and parameters are consistent with those reported by our research group before.<sup>[4]</sup>

#### 1.6.2 Simulation of GNRs:

To gain deeper insights into the mechanism of the chirality of the obtained CD signals, finite element method (FEM) simulations were carried out by using commercial software COMSOL Multiphysics software package. The CD signals were calculated as a difference in extinction of the left- and right-

circularly polarized light (*L*- and *R*-CPL). The assembled nanostructures were randomly dispersed in solution, and therefore we average the calculated values over the six directions of incident light. For simplicity, we used the GNRs-trimer as the model (illustrated in Fig. 3f). The GNRs were modeled with a diameter of 20 nm and the length of 60 nm. The refractive index was set as 1.40.

## 2. Characterization

### 2.1 Techniques

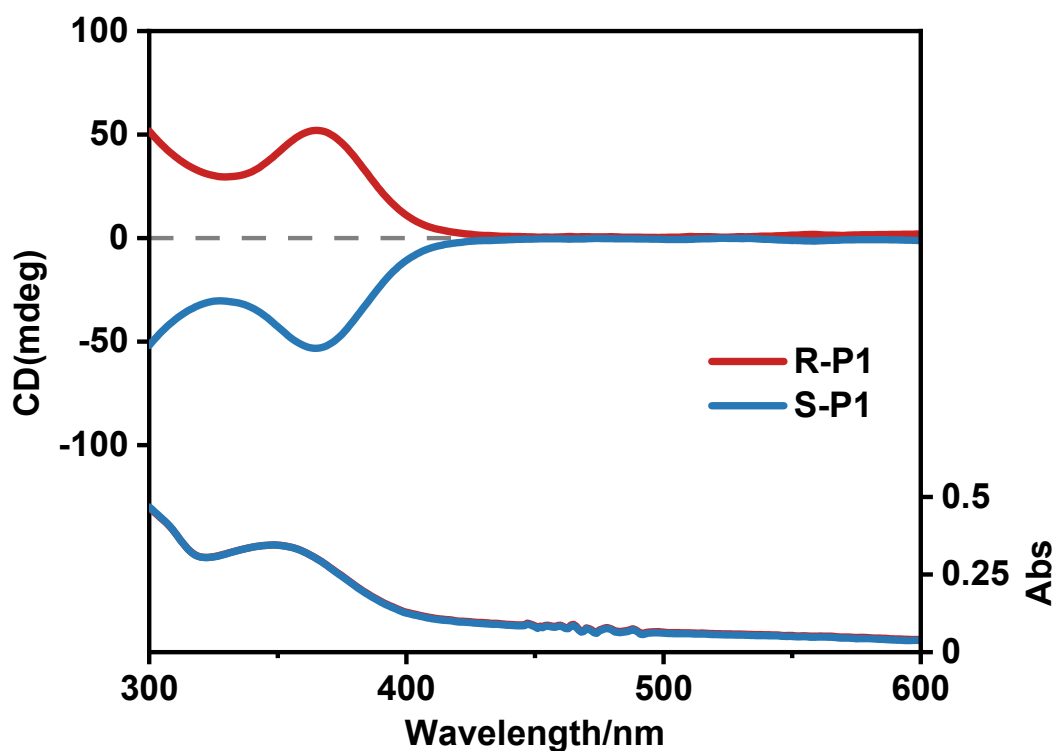
Circular dichroism (CD) spectra were obtained on a Jasco J-810 spectropolarimeter using THF as solvent at 25°C and analyzed by the associated J800 software. When the sample concentration was 0.4 mg/mL, using 0.5 mm cell (0.2 mg/mL: 1 mm cell, 0.1 mg/mL: 2 mm cell, 0.067 mg/mL: 3 mm cell, 0.04 mg/mL: 5 mm cell, 0.02 mg/mL: 10 mm cell). UV-Vis absorption measurements were carried out on a Varian Cary 1E UV-Vis spectrometer. Transmission electron microscope (TEM) images were obtained using Thermo Fisher Scientific (FEI) Tecnai T20 operating at 200 kV. The images were taken with Gatan Oneview IS camera. TEM samples were prepared by adding 10  $\mu$ l solution to the thin pure carbon film coated Cu grids of 300 mesh and blotting away the excess solution with dust-free paper. Dynamic light scatter (DLS) was carried out on a commercialized spectrometer nano Omni from Brookhaven Instrument Corporation. Scanning electron microscope (SEM) images were obtained on a Zeiss Merlin Compact field-emission scanning electron microscope operated at 10 KV. The samples were prepared by dipping a drop of solution onto hydrophilic cleaning silica wafers kept at 25 °C and the solutions were absorbed by dust-free paper after 15 s. The wafers were stuck to the conductive adhesive. Atomic force microscope (AFM) images were performed on a Bruker BioScope Resolve under ScanAsyst mode in the air. The ScanAsyst-Air probe was used and has one silicon tip on the nitride lever with a reflective Al back side. Scan rate 1 Hz, Peak Force Amplitude 150 nm, Peak Force Frequency 2 kHz. The AFM samples were prepared on silica wafers, the method of which is similar to the SEM ones. Vibrational circular dichroism (VCD) spectra were obtained on a Jasco FVS-6000 in a 0.15 mm CaF<sub>2</sub> cell. All VCD spectra were collected for 10 h at a resolution of 4 cm<sup>-1</sup>. Infrared spectra (IR) were performed on a Nicolet Fourier transform Magna-IR 750 spectrophotometer. Laser Raman spectra were recorded on a Thermo Scientific Nicolet NXR FT-Raman Spectrometer. Circularly polarized luminescence (CPL) spectra were carried out on a JASCO CPL-200 spectrofluoropolarimeter. An FLS980 Steady State & Time-resolved Fluorescence Spectrometer (Edinburgh Instruments Ltd.) was used to measure the photoluminescence intensity.

## 2.2 Supporting Figures

**Table S1.** Information of *R*-P1, P2, P3 and P4.

Sample <sup>a)</sup>	[M]/[I]	$M_n^b$ (kDa)	$\bar{D}$	DP	Yield <sup>c)</sup> (%)	$T_d^d$ (°C)
<i>R</i> -P1 <sub>44</sub>	120	69.8	1.09	44	61.1	341
<i>S</i> -P1 <sub>44</sub>	118	69.5	1.06	44	55.9	331
P2 <sub>34</sub>	120	54.3	1.16	34	66.3	337
P3 <sub>43</sub>	120	68.5	1.12	43	70.1	351
P4 <sub>451</sub>	500	1025	1.26	451	90.2	386

<sup>a.)</sup> 30 °C, THF. <sup>b.)</sup> Determined by SEC in THF using PS standards. <sup>c.)</sup> Isolated yields after purification from MeOH while all the conversion of monomers are above 99% determined by <sup>1</sup>H NMR. <sup>d.)</sup> 5% weight loss temperature under nitrogen at a heating rate of 10 °C/min.

**Figure S1.** CD and UV-vis spectra of *R*-P1 and *S*-P1 in THF,  $c_0 = 0.20$  mg/mL

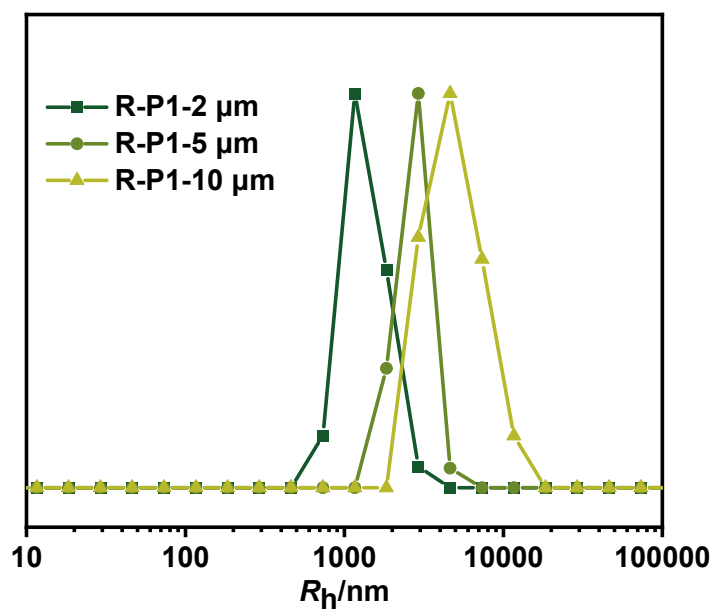
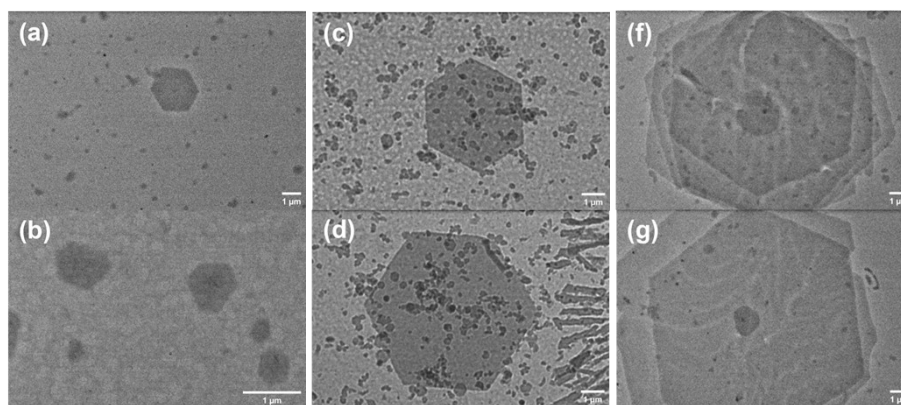


**Figure S2.** The TEM images of the **R-P1** in THF/EtOH solution ( $c_0 = 0.40$  mg/mL) with an average diameter of (a-b) 2 μm; (c-d) 5 μm and (f-g) 10 μm. (h) The  $R_h$  distributions of **P1** assemblies in the THF/ EtOH solution.

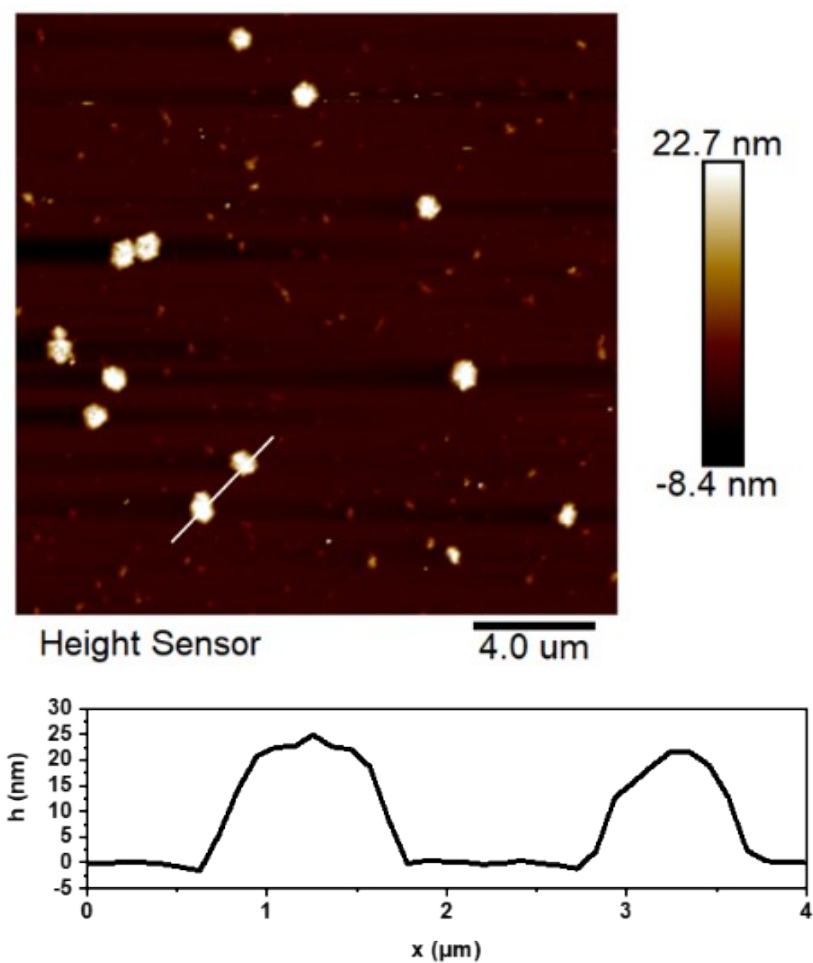


**Figure S3.** The AFM images as well as height analysis of P1 assemblies.

**Table S2.** The mean sizes of discrete GNRs with different aspect ratios.

Sample	Wavelength of the Longitudinal LSPR Peak/nm	Length/nm	Width/nm
G1	620	40±5	20±5
G2	660	60±5	20±5
G3	700	45±5	15±5
G4	720	80±5	20±5
G5	750	56±5	15±5
G6	520		20±1

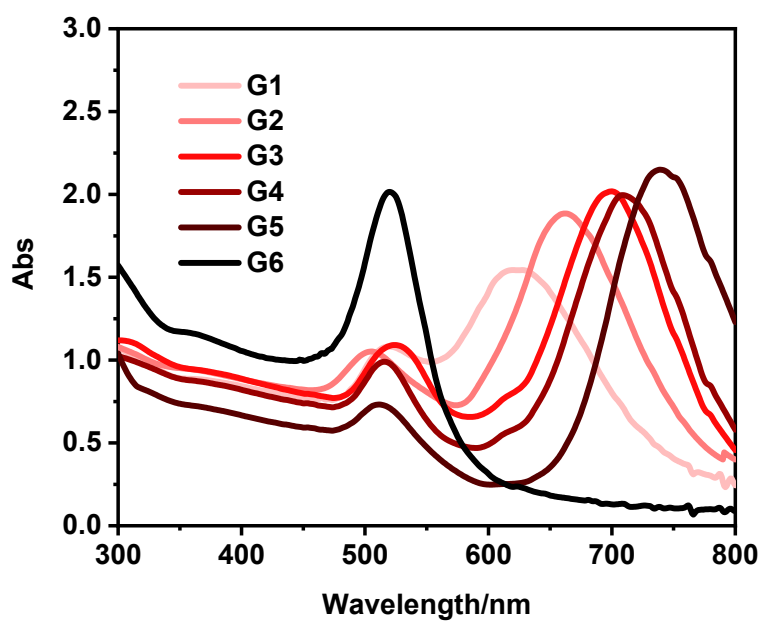


Figure S4. UV-Vis spectra of the GNRs.

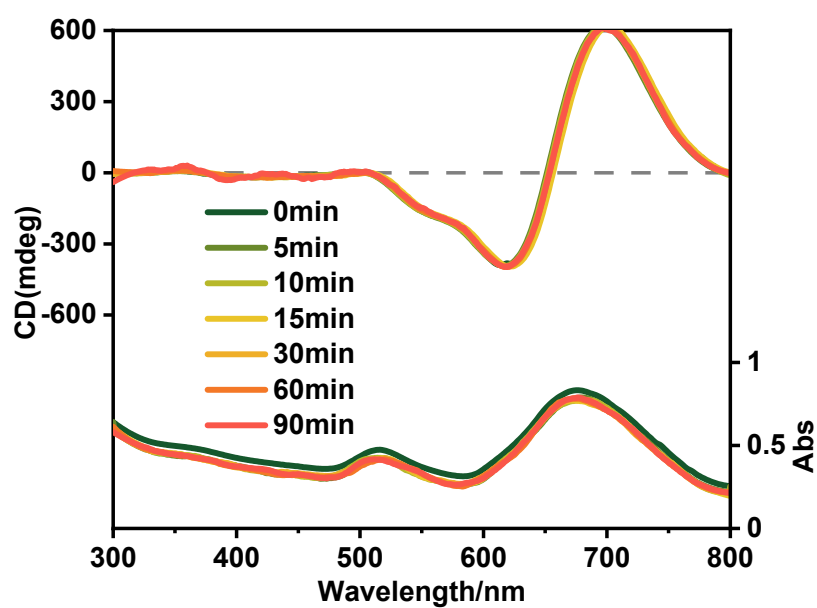
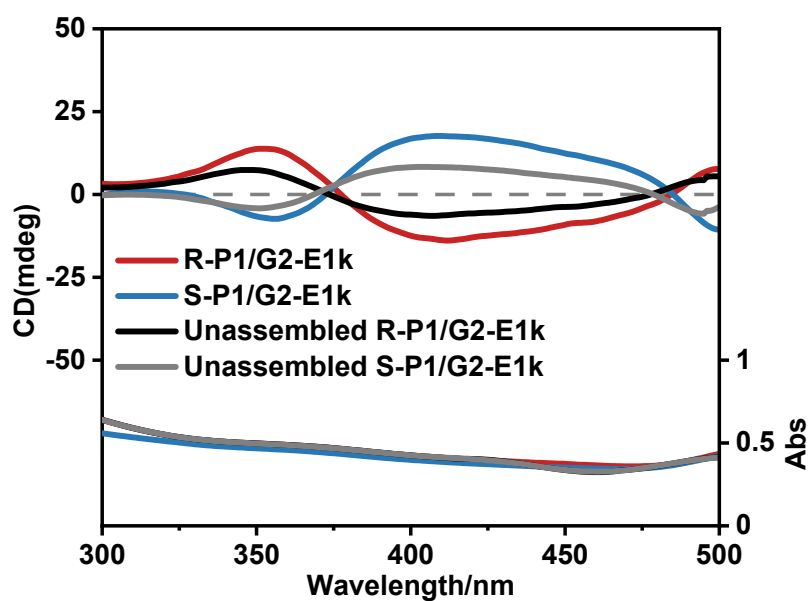
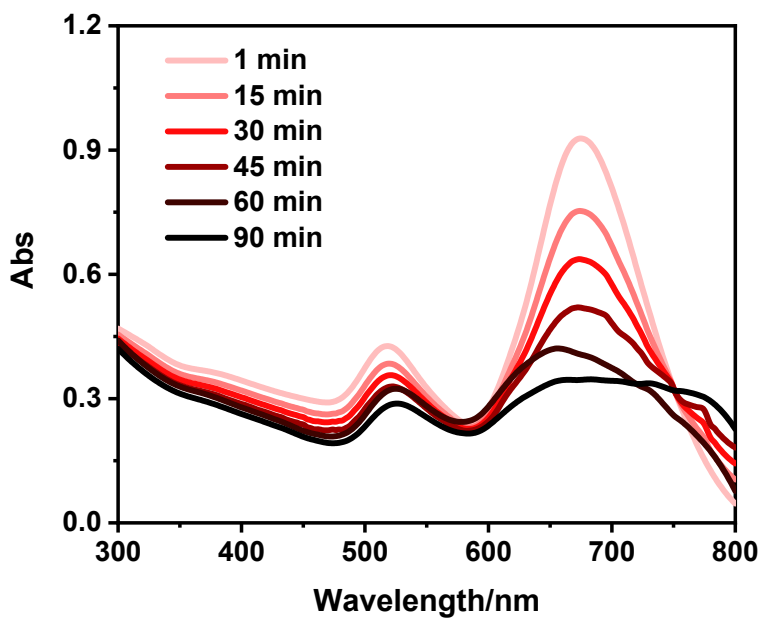


Figure S5. Time-dependent CD and UV-Vis spectra of R-P1/G2-E1k.



**Figure S6.** CD and UV-vis spectra of R-P1/G2-E1k and S-P1/G2-E1k. The CD and UV-vis of R-P1 and S-P1 are lower than those in Figure S1 because the thickness of the fluorescence cell used here is 1 mm, while 10 mm in Figure S1.



**Figure S7.** Time-dependent UV-Vis spectra of G2-E1k in THF.



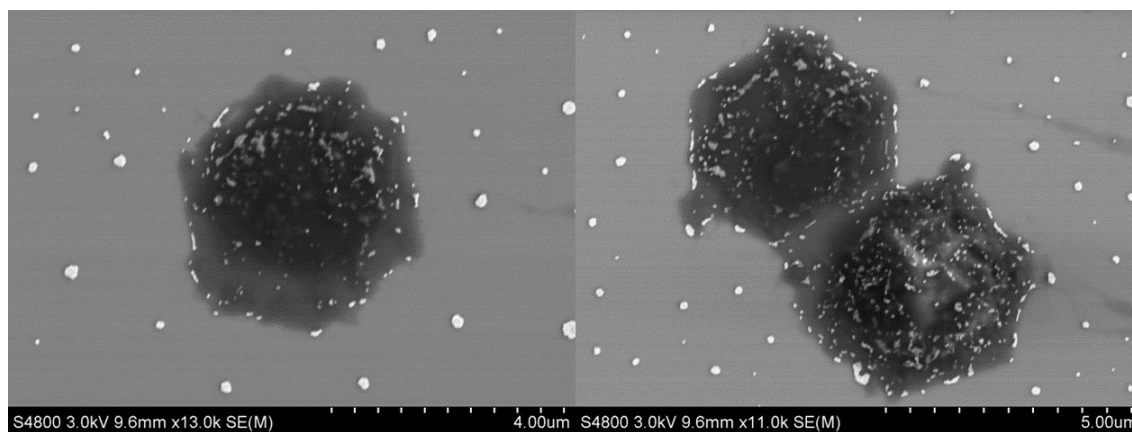


**Figure S8.** The SEM images of the *R-P1/G2-E1k* co-assemblies in THF/EtOH solution ( $c_0 = 0.40$  mg/mL).

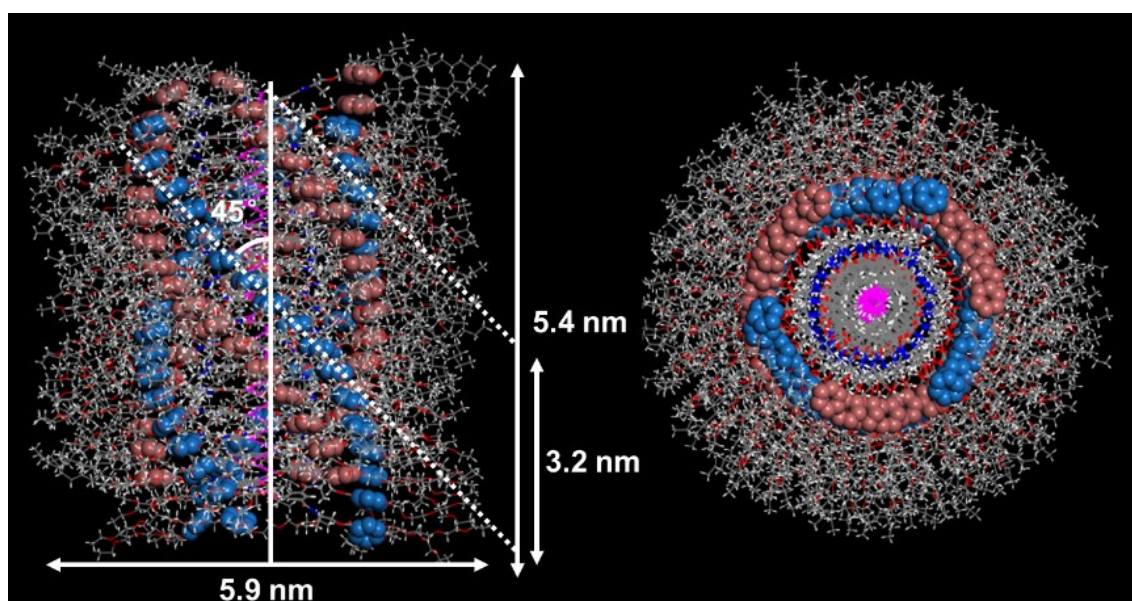


**Figure S9.** 3D models of *c-c R-P1* from the calculations at the dihedral angle  $\varphi \approx 40^\circ$ .

$$R_F = N^{3/5}a \quad \text{eq (1)}$$

**Equation S1.** The equation was used to calculate  $R_F$  of PEG, where  $a$  is the characteristic monomer dimension and  $N$  is the degree of polymerization.

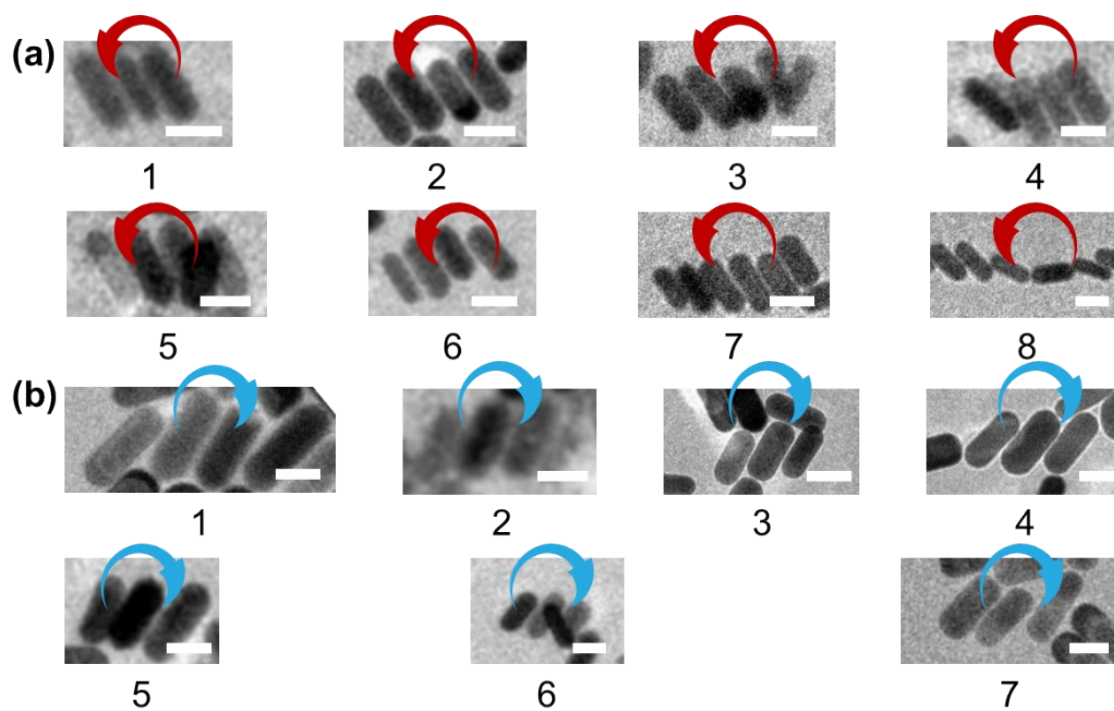


**Figure S10a.** The TEM images of *R-P1/G2-E1k* and *S-P1/G2-E1k* co-assemblies. (a) TYPE 1 of *R-P1/G2-E1k*. (b) TYPE 1 of *S-P1/G2-E1k*. Scale bars: 50 nm for TEM images.

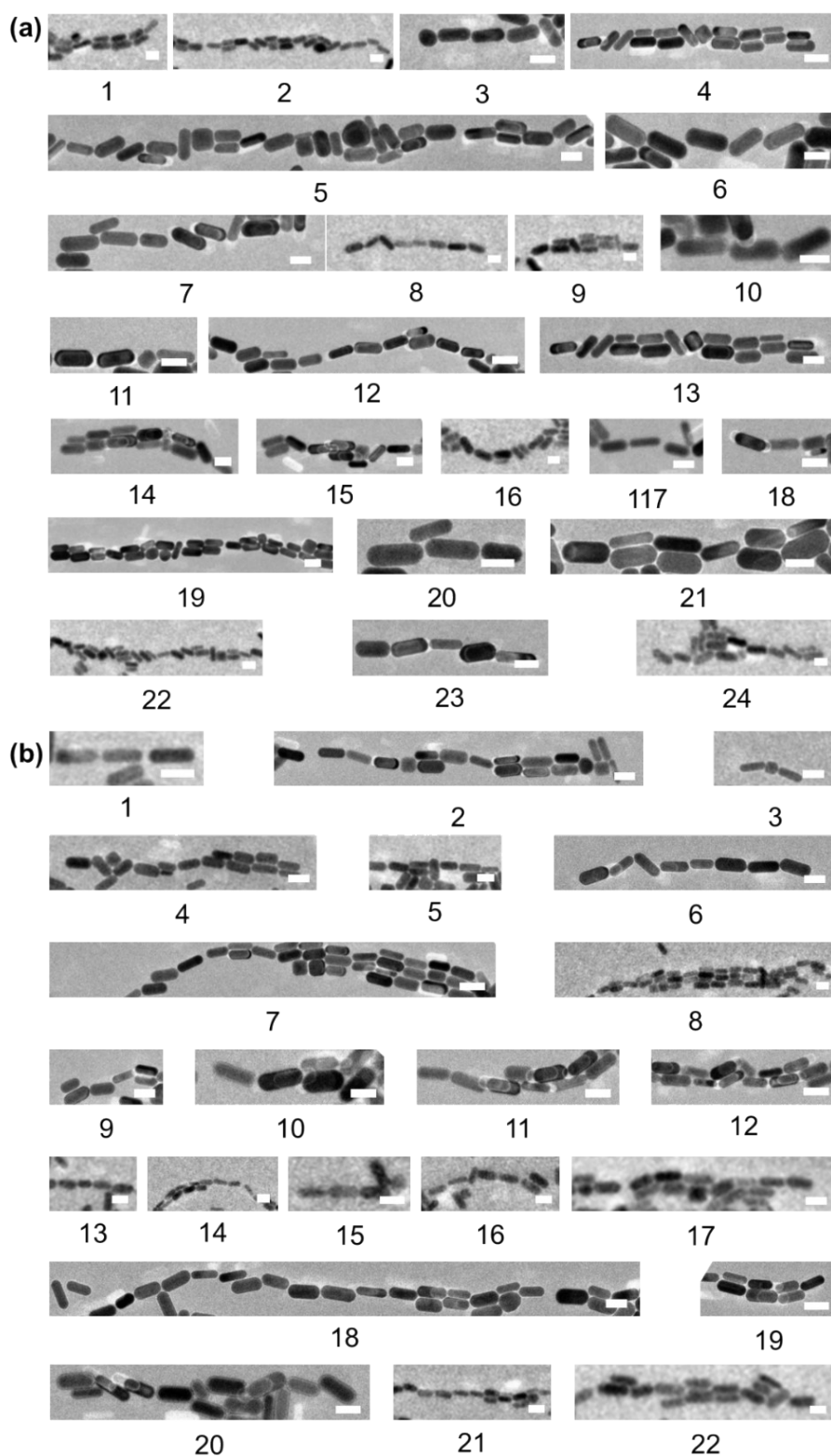


**Figure S10b.** The TEM images of *R-P1/G2-E1k* and *S-P1/G2-E1k* co-assemblies. (a) TYPE 2 of *R-P1/G2-E1k*. (b) TYPE 2 of *S-P1/G2-E1k*. Scale bars: 50 nm for TEM images.

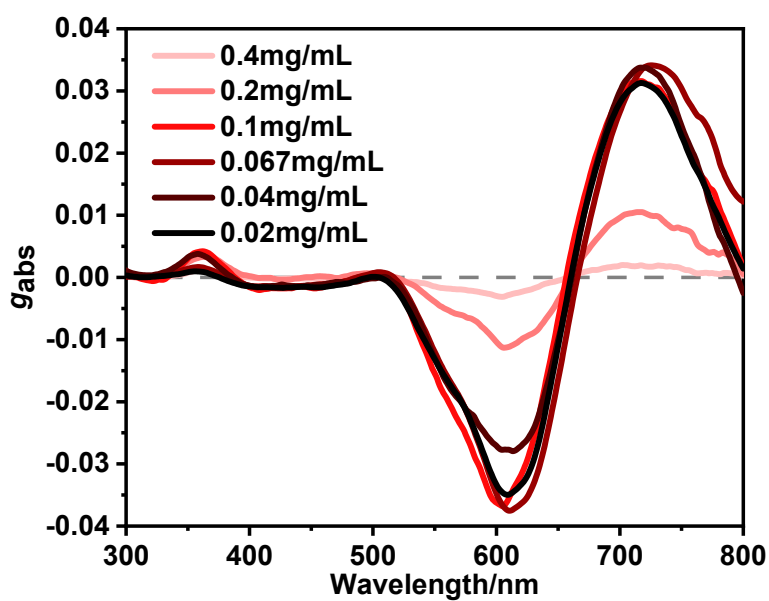


Figure S11. *g*-factor of R-P1/G2-E1k at different concentrations: 0.4-0.02 mg/mL.

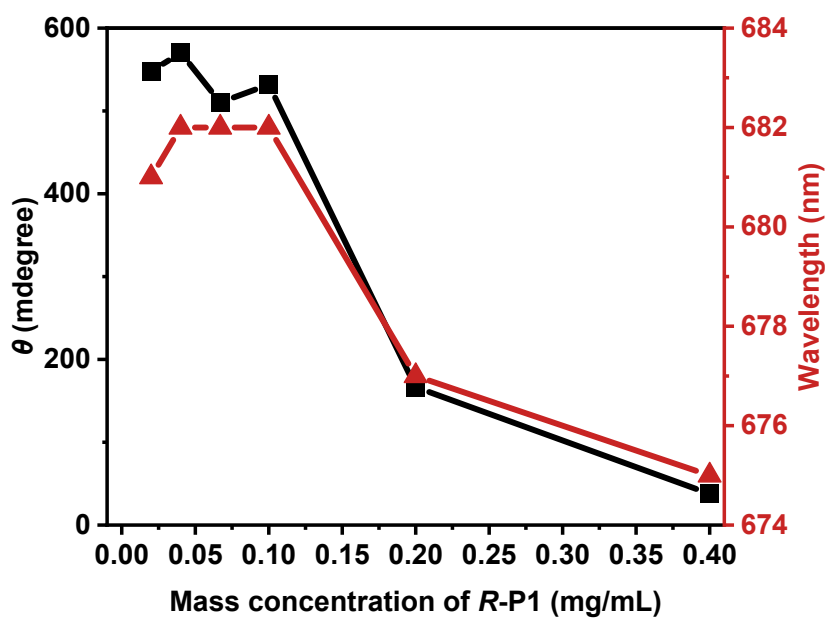
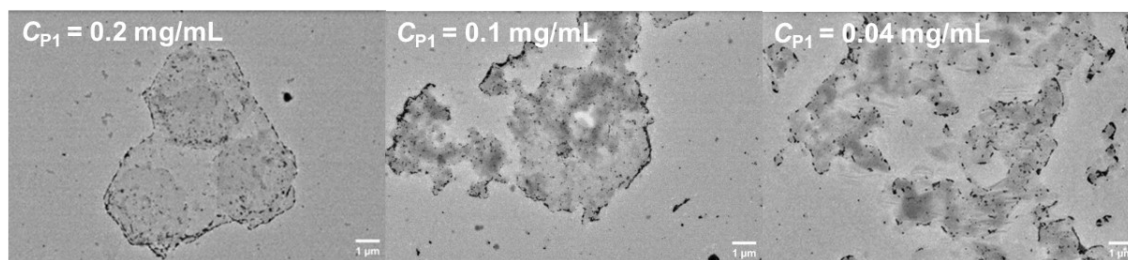
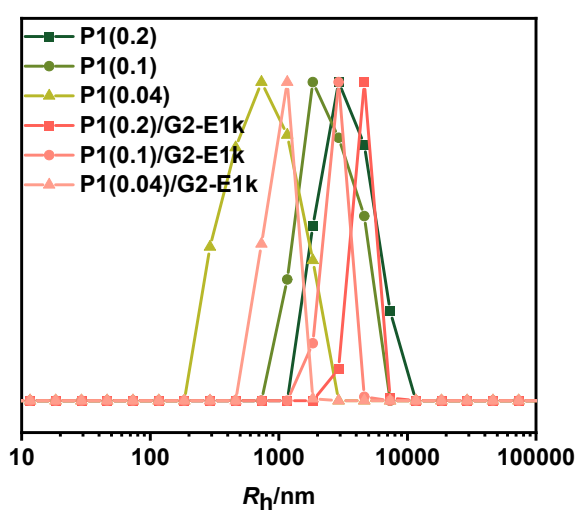


Figure S12. Peak value of PC signal and long-axis absorption peak value at different concentrations.



**Figure S13.** The TEM images of P1/G2-E1k at different concentrations.



**Figure S14.** The  $R_h$  distributions of R-P1/G2-E1k at different concentration in THF/EtOH.

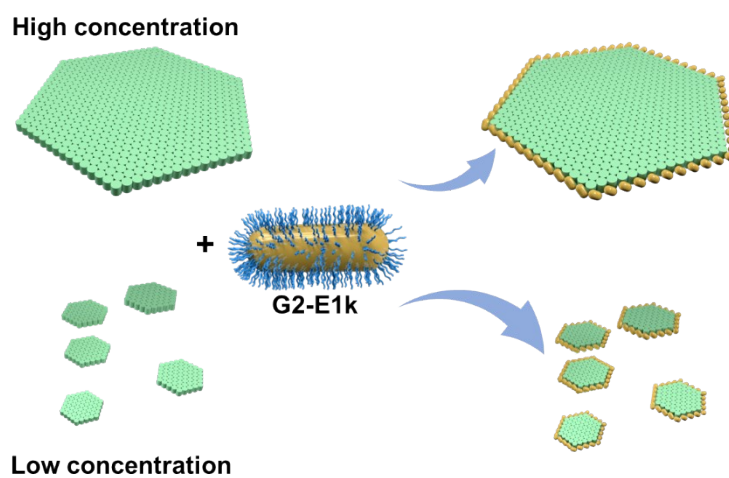


**Figure S15.** Schematic structure of R-P1/G2-E1k at different concentration of R-P1.

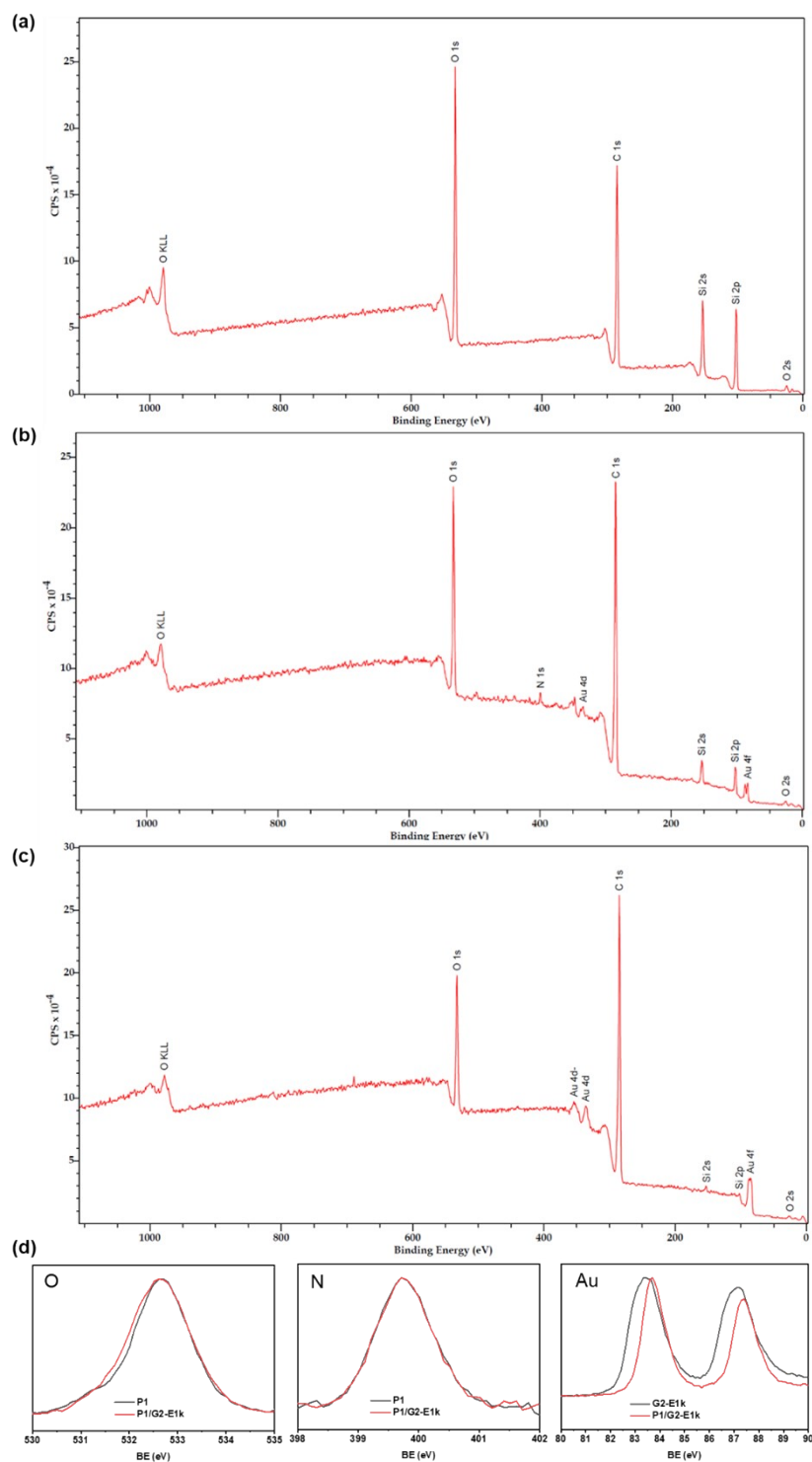


**Figure S16.** XPS spectra of *R-P1* (a), *R-P1/G2-E1k* (b) and *G2-E1k* (c). (d) Compare the XPS spectra before and after co-assembly.

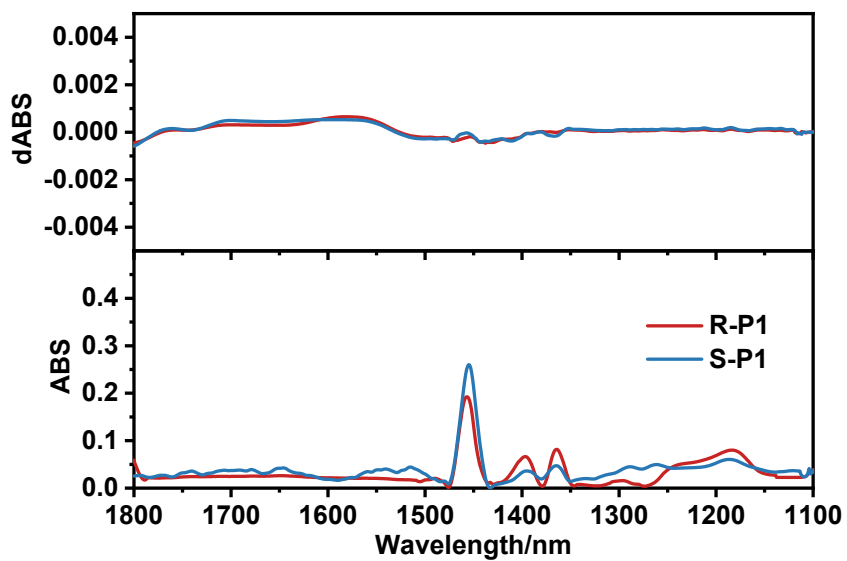


Figure S17. VCD spectra of R-P1 and S-P1 obtained from THF/EtOH.

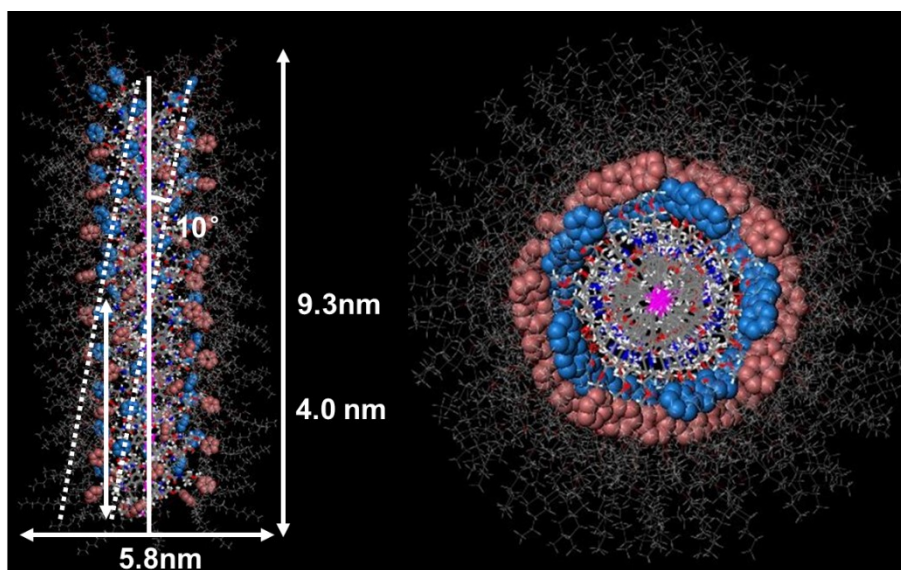
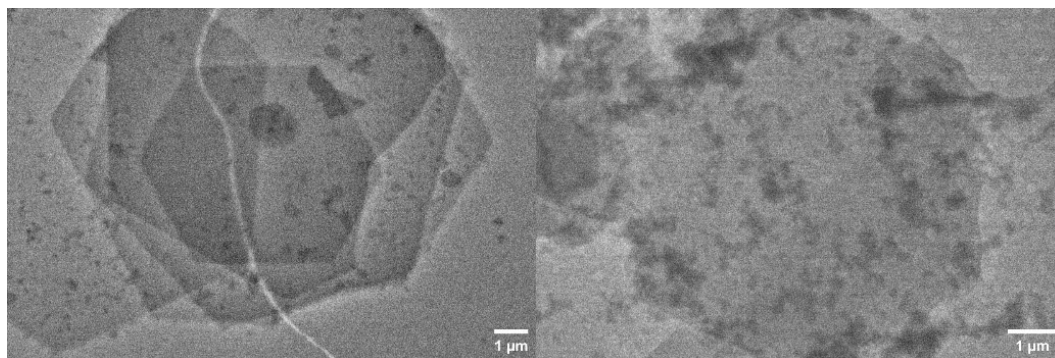
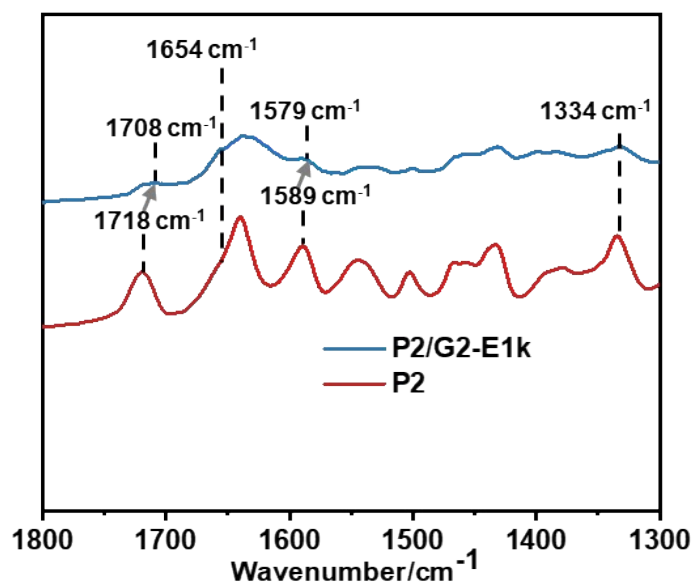


Figure S18. 3D models of *c-t* P2 from the calculations at the dihedral angle  $\varphi \approx -110^\circ$ .



**Figure S19.** The TEM images of the P2 in THF/EtOH solution ( $c_0 = 0.40$  mg/mL).



**Figure S20.** FT-IR spectra of P2 and P2/G2-E1k.



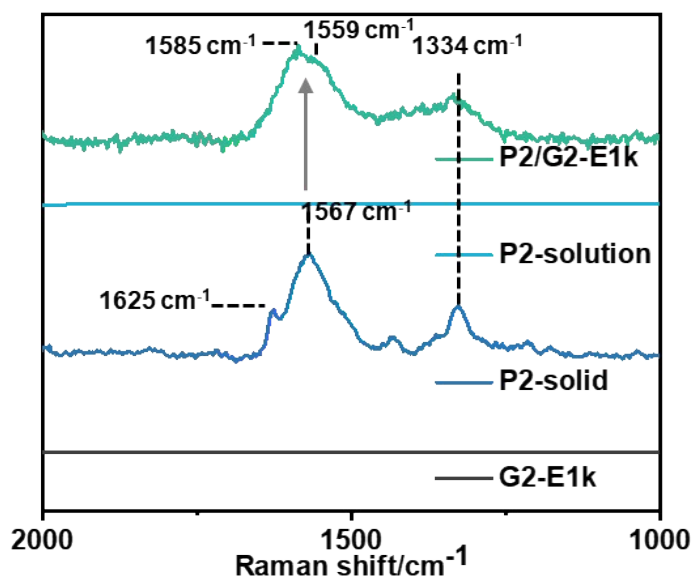


Figure S21. Raman spectra of G2-E1k, P2 and P2/G2-E1k obtained from THF/EtOH.

In simulation of GNRs, the tilt angle  $\theta$  ( $-90^\circ \leq \theta \leq 90^\circ$ ), is defined as the angle between the long axis of GNR and the Z-axis. The out-of-plane angle,  $\alpha$  ( $-90^\circ \leq \alpha \leq 90^\circ$ ), is defined as the angle between the long axis of GNR and the Z-X plane. We first consider the range of  $\alpha$ . When  $\alpha$  approaches  $90^\circ$ , the GNRs are nearly parallel to the X-Y plane, resulting in a very small area of non-covalent interaction between the GNRs and the PPA nanosheets. Therefore, we thought that the sides of GNRs are close to edges of nanosheets, and  $\alpha$  is small. The  $\alpha$  values of the out-of-plane angles of adjacent GNRs are the same, but with the opposite signs (for example, alternating at  $10^\circ$  and  $-10^\circ$ ).  $d$  is the distance between adjacent GNRs. The tilt angles  $\theta$  of R-P1/G2-E1k and P2/G2-E1k are set to  $-45^\circ$  and  $10^\circ$ , which are in consisted with the tilt angle of the helix in the assembled P1 and P2.

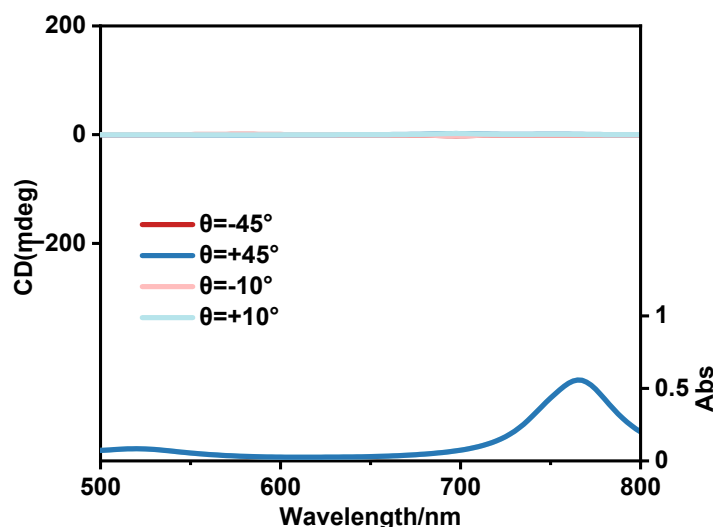
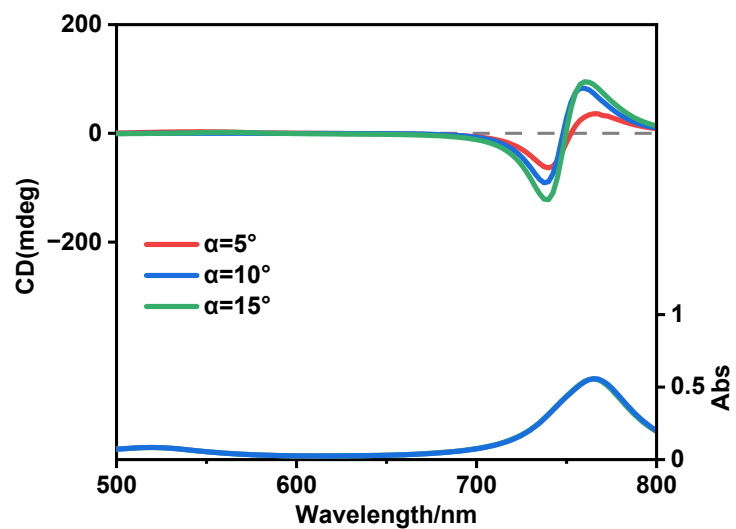
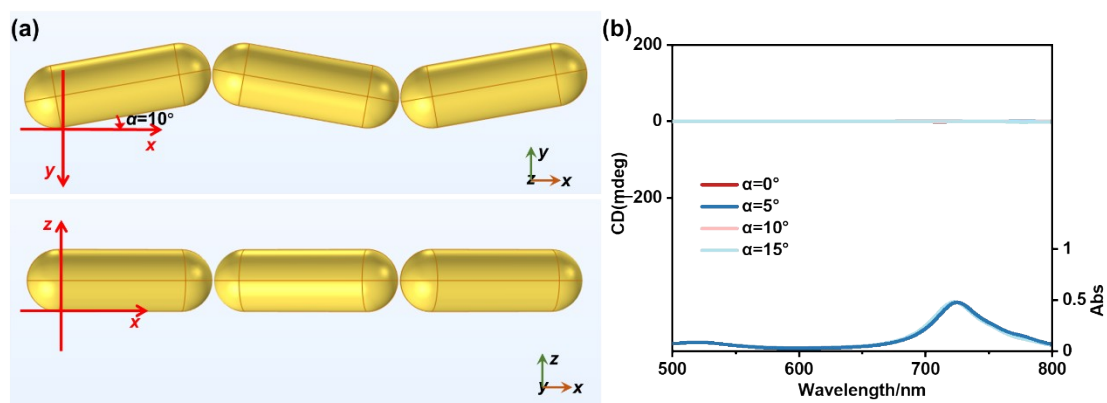


Figure S22. FDTD simulated CD and UV-Vis spectra.  $d = 15$  nm,  $\alpha = 0^\circ$ ,  $\theta = -45^\circ$  (R-P1/G2-E1k),  $-10^\circ$ ,  $+10^\circ$  (P2/G2-E1k) and  $+45^\circ$  (S-P1/G2-E1k).



**Figure S23.** FDTD simulated CD and UV-Vis spectra.  $d = 15$  nm,  $\vartheta = -45^\circ$  (**R-P1/G2-E1k**),  $\alpha = 5^\circ, 10^\circ$  and  $15^\circ$ .



**Figure S24** (a) Schematic structures of EE arrangement,  $\vartheta = 90^\circ$ ; (b) FDTD simulated CD and UV-Vis spectra.  $d = 60$  nm,  $\vartheta = 90^\circ$  (**R-P1/G2-E1k**),  $\alpha = 0^\circ, 5^\circ, 10^\circ$  and  $15^\circ$ .

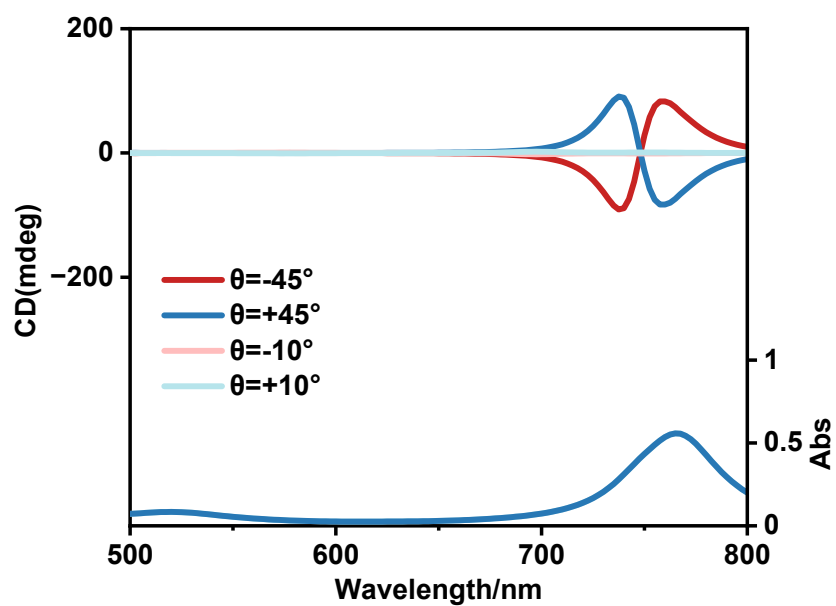


Figure S25. FDTD simulated CD and UV-Vis spectra.  $d = 5$  nm,  $\alpha = 10^\circ$ ,  $\vartheta = -45^\circ$  (*R*-P1/G2-E1k),  $-10^\circ$ ,  $+10^\circ$  (*P*2/G2-E1k) and  $+45^\circ$  (*S*-P1/G2-E1k).

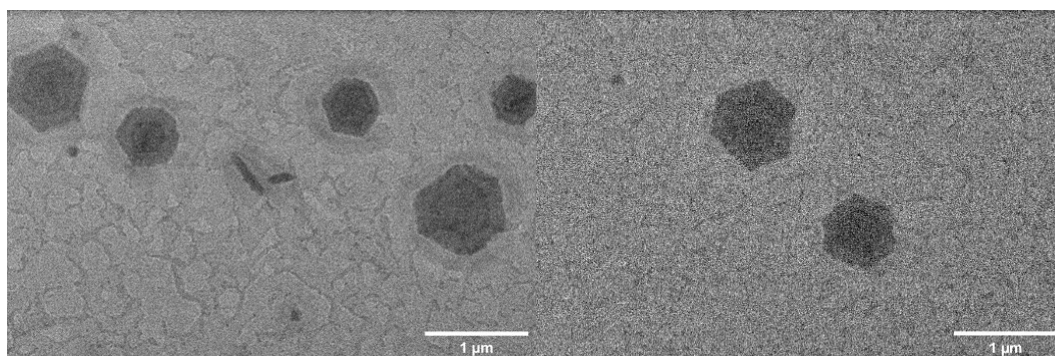


Figure S26. The TEM images of the **P3** in THF/EtOH solution ( $c_0 = 0.40$  mg/mL).

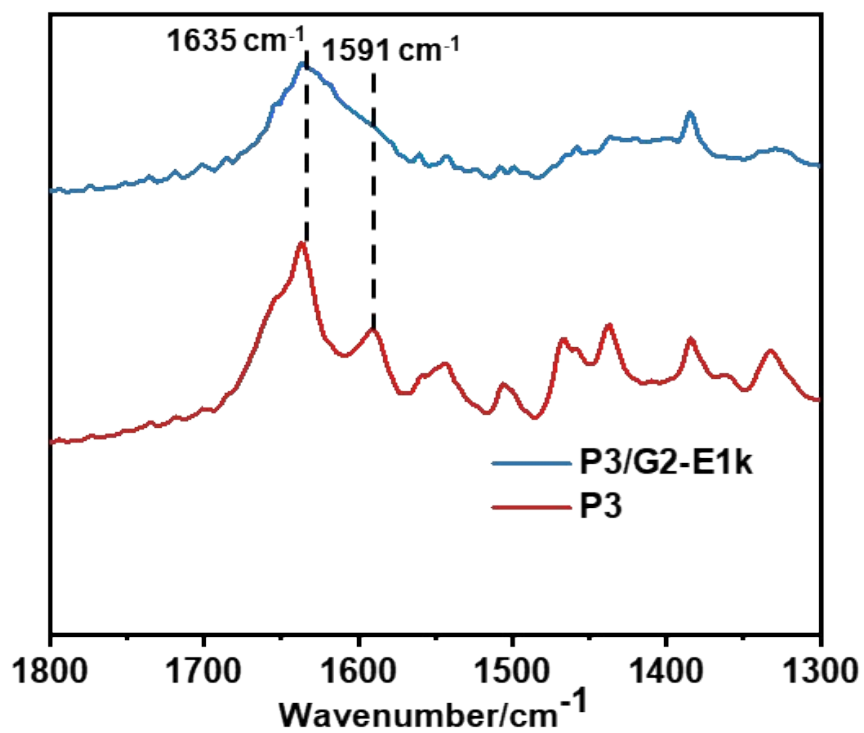
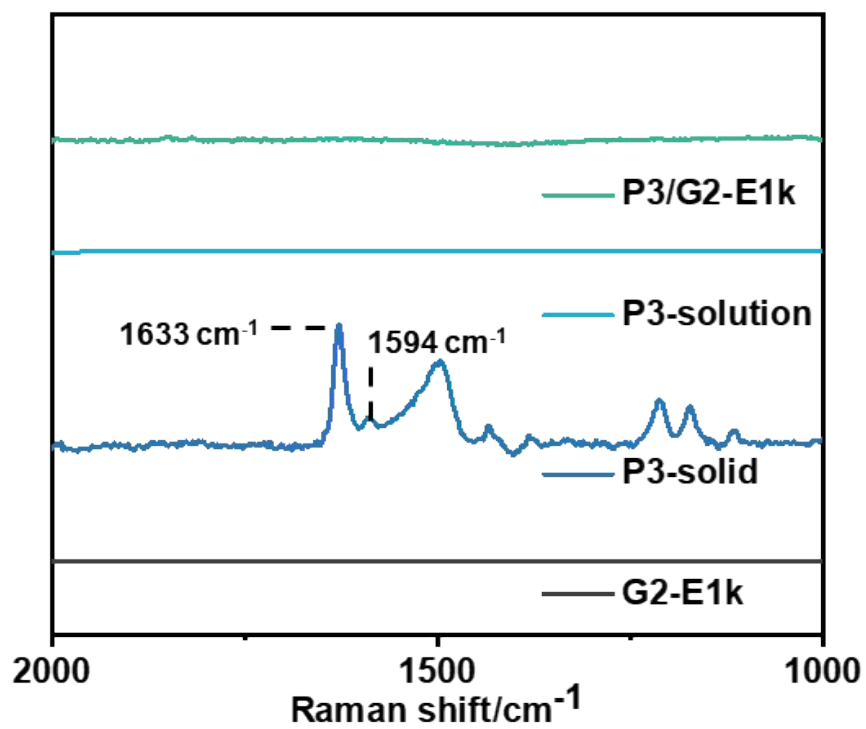
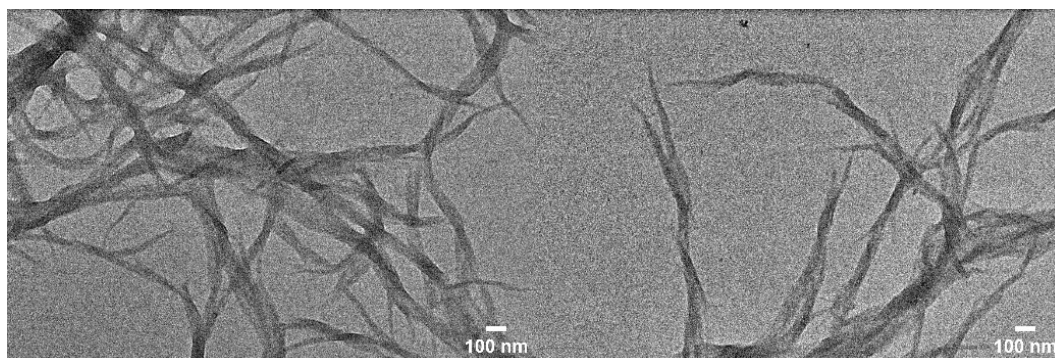


Figure S27. FT-IR spectra of P3 and P3/G2-E1k.



**Figure S28.** Raman spectra of G2-E1k, P3 and P3/G2-E1k obtained from THF/EtOH.



**Figure S29.** The TEM images of the P4 in THF/EtOH solution ( $c_0 = 0.15$  mg/mL).

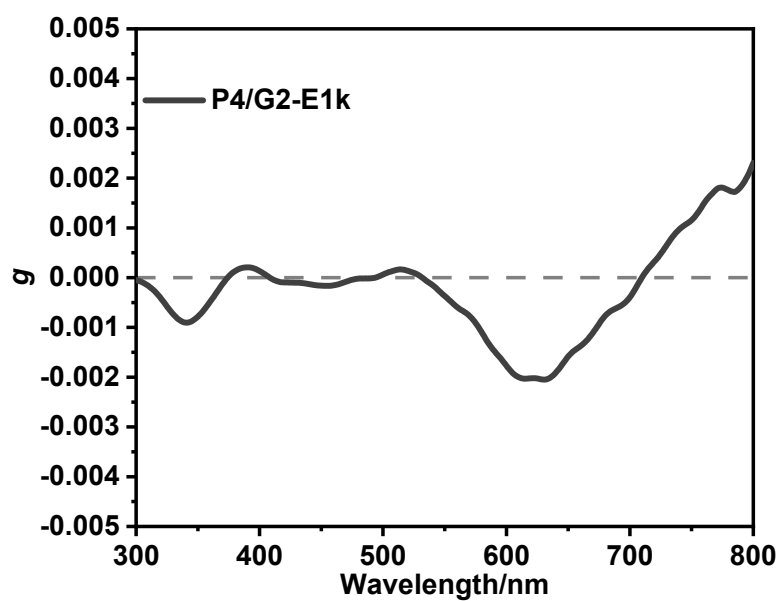


Figure S30. g-factor of P4/G2-E1k.

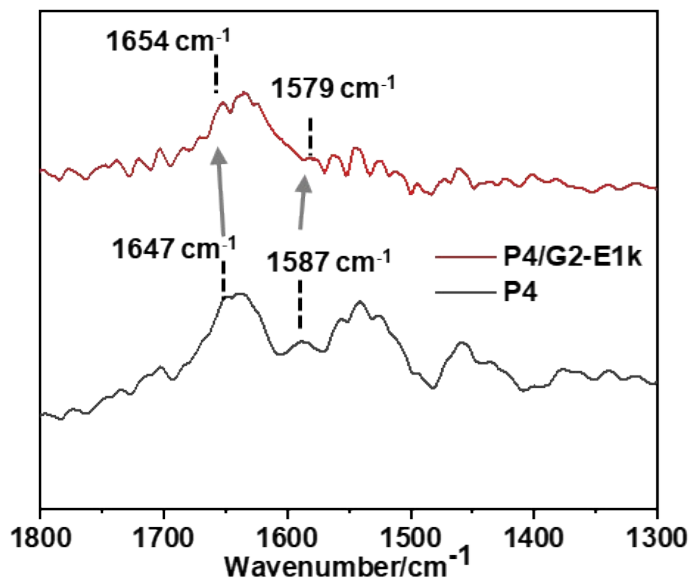


Figure S31. FT-IR spectra of P4 and P4/G2-E1k.

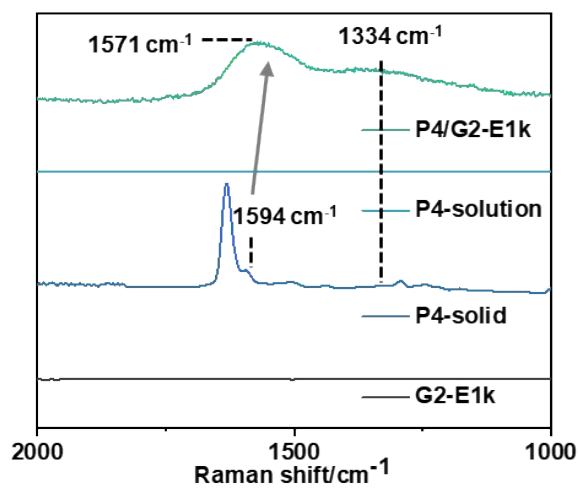


Figure S32. Raman spectra of G2-E1k, P4 and P4/G2-E1k obtained from THF/EtOH.

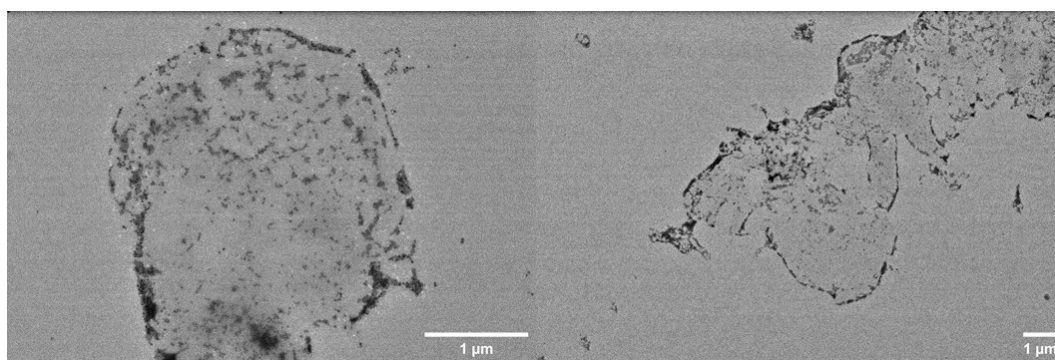


Figure S33. The TEM images of R-P1/G6-E1k co-assemblies.

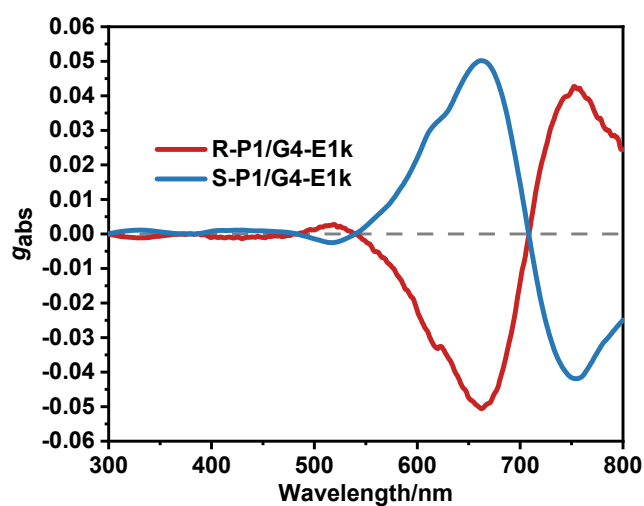
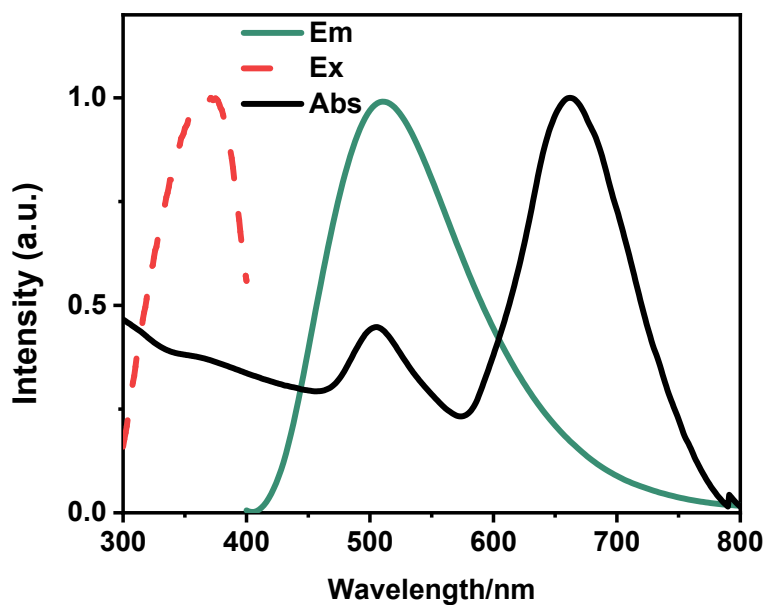


Figure S34. The g-Value of R-P1/G4-E1k and S-P1/G4-E1k.



**Figure S35.** The fluorescence spectra of *R-P1* assemblies in THF/EtOH solution ( $c_0 = 0.4$  mg/mL) and UV-Vis spectra of *G2-E1k*.

## References

1. B. Nikoobakht, M. A. El-Sayed, *Chem. Mater.* **2003**, *15*, 1957.
2. Z. Zhu, W. Liu, Z. Li, B. Han, Y. Zhou, Y. Gao, Z. Tang, *ACS Nano* **2012**, *6*, 2326.
3. W. Yan, L. Xu, C. Xu, W. Ma, H. Kuang, L. Wang, N. A. Kotov, *J. Am. Chem. Soc.* **2012**, *134*, 15114.
4. S. Cai, Y. Huang, S. Xie, S. Wang, Y. Guan, X. Wan, J. Zhang, *Angew. Chem. Int. Ed.* **2022**, *61*, e202214293.
5. S. Wang, S. Xie, H. Zeng, H. Du, J. Zhang, X. Wan, *Angew. Chem. Int. Ed.* **2022**, *134*, e202202268.